Tensor-Based Framework With Model Order Selection and High Accuracy Factor Decomposition for Time-Delay Estimation in Dynamic Multipath Scenarios

MATEUS DA ROSA ZANATTA[1], (Graduate Student Member, IEEE),
JOÃO PAULO CARVALHO LUSTOSA DA COSTA[1,6], (Senior Member, IEEE),
FELIX ANTREICH[2], (Senior Member, IEEE),
MARTIN HAARDT[3], (Fellow, IEEE), **GORDON ELGER**[4,5,6],
FÁBIO LÚCIO LOPES DE MENDONÇA[1],
AND RAFAEL TIMÓTEO DE SOUSA, JR.[1], (Senior Member, IEEE)

[1]Department of Electrical Engineering, University of Brasilia, Brasília 70910-900, Brazil
[2]Department of Telecommunications, Aeronautics Institute of Technology (ITA), São José dos Campos 12227-010, Brazil
[3]Communications Research Laboratory, Technische Universität Ilmenau, 98693 Ilmenau, Germany
[4]Faculty of Electrical Engineering and Information Technology, Technische Hochschule Ingolstadt, 85049 Ingolstadt, Germany
[5]Fraunhofer Institute for Transportation and Infrastructure Systems IVI, Application Center Connected Mobility and Infrastructure Stauffenbergstraße 2a,
D-85051 Ingolstadt, Germany
[6]Hochschule Hamm-Lippstadt, 59557 Lippstadt, Germany

Corresponding author: Mateus da Rosa Zanatta (mateus.zanatta@redes.unb.br)

ABSTRACT Global Navigation Satellite Systems (GNSS) are crucial for applications that demand very accurate positioning. Tensor-based time-delay estimation methods, such as CPD-GEVD, DoA/KRF, and SECSI, combined with the GPS3 L1C signal, are capable of, significantly, mitigating the positioning degradation caused by multipath components. However, even though these schemes require an estimated model order, they assume that the number of multipath components is constant. In GNSS applications, the number of multipath components is time-varying in dynamic scenarios. Thus, in this paper, we propose a tensor-based framework with model order selection and high accuracy factor decomposition for time-delay estimation in dynamic multipath scenarios. Our proposed approach exploits the estimates of the model order for each slice by grouping the data tensor slices into sub-tensors to provide high accuracy factor decomposition. We further enhance the proposed approach by incorporating the tensor-based Multiple Denoising (MuDe).

INDEX TERMS Global navigation satellite systems (GNSS), global positioning system (GPS), GPS3, time-delay estimation (TDE), multipath components, model order selection (MOS).

I. INTRODUCTION

As Global Navigation Satellite Systems (GNSS) become more ubiquitous and this technology proved to be essential

for applications such as civilian aviation, autonomous driving, defense, and timing and synchronization of critical networks. GNSS receivers require line of sight (LOS) signals from at least four satellites to estimate their position on the Earth's surface. Additionally, besides the LOS component, non-LOS (NLOS) multipath components are received

due to the reflections on trees, poles, lamps, and buildings. Therefore, the superposition of the LOS and NLOS multipath components degrades the time-delay estimation (TDE) and, consequently, the positioning estimation.

State-of-the-art GNSS receivers equipped with a single antenna are in general remarkably sensitive to the effect of multipath components [1]–[3]. Thus, multi-antenna GNSS receivers became the focus of research on resilient positioning withstanding not only multipath but also interference and spoofing. In addition to beamforming approaches [4], [5], multi-dimensional parameter estimation approaches [6], [7], and other approaches as those proposed in [8] and [9], tensor-based decomposition methods showed significant improvements over matrix-based decomposition methods. A tensor-based decomposition features uniqueness, improves the identifiability of the parameters, and the tensor structure permits efficient denoising of the received signal. Therefore, tensor-based multipath mitigation methods, combined with antenna arrays, have been proposed as an alternative to single antenna and matrix-based techniques.

In [10], the authors propose a so-called Tensor-based Eigenfilter using the Higher-Order Singular Vector Decomposition (HOSVD) combined with Forward-Backward Averaging (FBA) [11], Spatial Smoothing (SPS) [12], [13], and a bank of correlators to mitigate multipath and to improve time-delay estimation of the LOS signal. In [14] a three step approach based on direction of arrival (DoA) estimation, the Khatri-Rao factorization (KRF), and a bank of correlators was proposed. This DoA/KRF method [14] outperforms traditional matrix-based decomposition methods. However, the performance of this approach depends on estimates of the DoAs of the received signals to construct the respective loading matrices of the signal tensor decomposition. Furthermore, [14] assumes a static environment, thus it cannot be applied to scenarios where the model order changes over-time. In [15], the authors proposed the Canonical Polyadic Decomposition by a Generalized Eigenvalue Decomposition (CPD-GEVD). Although the CPD-GEVD showed robustness in the presence of multipath components and array imperfections, it assumes a constant model order between data epochs. In [16], the tensor-based methods proposed in [10], [14], [15] were extended to third-generation GPS (GPS3) signals, since GPS3 is more robust against multipath components in comparison to the signals of the second-generation GPS (GPS2) due to its Time Multiplexed Binary Offset Carrier (TMBOC) modulation [17]–[19]. In [20], the authors showed that the SEmi-algebraic framework for computing an approximate CP decomposition via Simultaneous Matrix Diagonalizations (SECSI) [21] can be applied to GPS2 and GPS3 signals and antenna array-based receivers using GPS3 and SECSI outperform antenna array receivers using GPS2 and SECSI. This underlines the superior multipath performance of the new GPS3 signals. Additionally, [20] showed that the SECSI method is more robust in the presence of strongly correlated signals than the CPD-GEVD method while on the other hand being computationally more expensive.

The Tensor-based Eigenfilter [10] does not require a previous model order selection (MOS), but achieves lower accuracy compared to the methods proposed in [15], [20]. However, the CPD-based techniques, introduced in [15], [20], require an estimate of the tensor model order to enable tensor factorization. Thus, even though [15], [20] have improved the performance of TDE in presence of highly correlated multipath, these methods assume a known and constant model order. Recently, in [22], the authors proposed the $(L_r, L_r, 1)$-GEVD approach to perform multi-linear rank-$(L_r, L_r, 1)$ decomposition by clustering NLOS components and obtaining the LOS component. Meanwhile, in [23], the authors proposed a tensor-based subspace tracking framework to keep track and update the tensor signal subspace. However, similarly to previous tensor-based methods, [22] and [23] assume that the model order is constant between data epochs. Hence, MOS schemes need to be included and assessed for the application of tensor-based methods for GNSS in order to achieve highly accurate and robust TDE of the LOS signal in case correlated multipath signals are received.

The literature on MOS for matrix data models is quite extensive. The following approaches can be considered the state-of-the art of matrix-based MOS: 1-D Akaike's Information Criterion (AIC) [24], 1-D Minimum Description Length (MDL) [24], EFT [25], Modified EFT (M-EFT) [24], RADOI [26], and the subspace-based ESTER [27]. Also, tensor-based MOS was proposed as well, such as R-D AIC [28], R-D MDL [28], and R-D EFT [24]. Even though MOS methods are crucial to mitigate multipath components, the literature hardly investigates MOS methods for GNSS applications. For example, in [29], the authors apply MDL with antenna arrays to estimate GNSS NLOS components, thus showing that the model order estimation depends on the carrier-to-noise density ratio (C/N_0) of the received signals. Furthermore, in [30], a multipath detection algorithm is developed based on a one-way analysis of the variance (ANOVA). However, in [30], the authors assume the DOA of the LOS signal to be known.

In this paper, we propose a tensor-based framework with model order selection and high accuracy factor decomposition for TDE in dynamic multipath scenarios for GNSS. This new approach includes the estimation of the model order for each slice of the data tensor and subsequent grouping of the data tensor into sub-tensors. To successively apply SPS, denoising, and reconstruction of the noisy data, the proposed high accuracy tensor-based decomposition, uses the respective sub-tensors combined to the tensor-based MUltiple DEnoising (MuDe) [31]. Therefore, the proposed framework is composed of four steps, namely, estimation of the number of multipath components in slow and fast dynamic multipath scenarios, further mitigation of the multipath effect by employing the tensor-based MuDe, separation of the sources by using our proposed high accuracy tensor-based decomposition exploiting the different model orders of the slices of the data tensor, and estimation of the time-delay of the signal components.

This paper has six sections, including this introduction. Section II introduces the notation utilized in the paper. In Section III, the data model assuming multipath components and the dynamic model order is presented. Section IV describes the proposed tensor-based framework with model order selection and multiple denoising for dynamic multipath components. Section V presents and discusses simulation results for the proposed framework. Section VI draws the conclusions.

II. NOTATION

In this section, we introduce the mathematical notation used in this paper. Scalars are represented by italic letters (a, b), vectors by lowercase bold letters (**a**, **b**), matrices by uppercase bold letters (**A**, **B**), and tensors by uppercase bold calligraphic letters ($\mathcal{A}$, $\mathcal{B}$). The superscripts $^{\mathrm{T}}$, *, $^{\mathrm{H}}$, $^{-1}$, and $^{+}$ denote the transpose, conjugate, conjugate transpose (Hermitian), the inverse of a matrix, and pseudo-inverse of a matrix, respectively.

Additionally, for a vector $\mathbf{a} \in \mathbb{C}^{N}$, the nth element is denoted as a_n. Moreover, for a matrix $\mathbf{A} \in \mathbb{C}^{M \times N}$, the element in the mth row and nth column is denoted by $a_{m,n}$, its mth row is denoted by $\mathbf{A}_{m,\cdot}$, and its nth column is denoted by $\mathbf{A}_{\cdot,n}$. Furthermore, the vec$\{\cdot\}$ operator reshapes a matrix into a vector by stacking all elements in a column vector. The operators $\diamond$ and $\circ$ denote the Khatri-Rao product and the outer product, respectively.

The operator cond$\{\cdot\}$ computes the condition number of a matrix. The smaller is the condition number, the more is stable the inverse, of the said matrix [32]. The Frobenius norm of a matrix $\mathbf{A}$ is denoted by $||\mathbf{A}||_{\mathrm{F}}$ whereas $||\mathbf{A}_{\cdot,n}||_2$ is the vector norm. For a matrix $\mathbf{A} \in \mathbb{C}^{M \times N}$ with $M < N$, the diag$\{\cdot\}$ operator extracts the diagonal of a matrix.

The n-mode unfolding of tensor $\mathcal{A}$ is denoted as $[\mathcal{A}]_{(n)}$, which is the matrix form of $\mathcal{A}$ obtained by varying the nth index along the rows and stacking all other indices along the columns of $[\mathcal{A}]_{(n)}$. The n-mode product between tensor $\mathcal{A}$ and a matrix $\mathbf{B}$ is represented as $\mathcal{A} \times_n \mathbf{B}$. The Nth order $\mathcal{I}_{N,L} \in \mathbb{R}^{L \times \dots L}$ is defined as the N-way identity tensor of size L, whose elements are equal to one if the N indices are equal and zero, otherwise.

III. DATA MODEL

This section firstly introduces the scenario considered in this work in Subsection III-A. Subsection III-B describes how the signal tensor is constructed. Finally, in Subsection III-C, the post-correlation data model is defined for a GPS L1C pilot signal [17].

A. SCENARIO

We consider a GNSS receiver equipped with an antenna array with M elements. We assume that for the received signals of $d = 1, \dots, D$ satellites, the LOS signal of the dth satellite is superimposed with $L_{d_{(k)}} - 1$ NLOS multipath components. The observations are collected during K periods (or epochs) each with N samples, where $k = 1, \dots, K$ and

$n = 1, \dots, N$. Moreover, the total number of received signal components is $L_{(k)} = \sum_{d=1}^{D} L_{d_{(k)}}$, where $\ell_{(k)} = 1, \dots, L_{(k)}$ and $\ell_{d_{(k)}} = 1, \dots, L_{d_{(k)}}$ are the ℓth and ℓ_dth component at the kth epoch. Furthermore, we assume that $\tau_1^{(d)}$ is the time-delay of the LOS component of the dth satellite, while $\tau_2^{(d)}, \dots, \tau_{L_{d_{(k)}}}^{(d)}$ are the time-delays of the $(L_{d_{(k)}} - 1)$ non-LOS (NLOS) components. Each satellite broadcasts the L1C pilot signal with carrier frequency $f_c = 1575.42$ MHz. The received signals are down-converted to baseband and sampled at a sampling rate of $f_s = 2B$, where B is the one-sided signal bandwidth.

B. PRE-CORRELATION DATA MODEL

As shown in [15], a tensor model can be used to express the received complex baseband signal at the output of the M antennas of an antenna array as

$$\mathcal{X} = \mathcal{I}_{3,L} \times_1 \tilde{\Gamma}^{\mathrm{T}} \times_2 \tilde{\mathbf{C}}^{\mathrm{T}} \times_3 \tilde{\mathbf{A}} + \mathcal{N} \quad (1)$$

where

$$\tilde{\Gamma}^{\mathrm{T}} = [\boldsymbol{\gamma}_1, \dots, \boldsymbol{\gamma}_{L(k)}] \in \mathbb{C}^{K \times L_{(k)}} \quad (2)$$

collects the complex amplitudes of each signal component during K epochs with

$$\boldsymbol{\gamma}_\ell \in \mathbb{C}^{K \times 1} = [\gamma_1, \dots, \gamma_K]^{\mathrm{T}} \quad (3)$$

including the complex amplitudes at each epoch. The matrix

$$\tilde{\mathbf{C}} = \Big[\mathbf{c}_1[\tau_1^{(1)}], \dots, \mathbf{c}_1[\tau_{\ell_{1(k)}}^{(1)}], \dots, $$
$$\mathbf{c}_D[\tau_{\ell_{d_{(k)}}}^{(D)}], \dots, \mathbf{c}_D[\tau_{L_{d_{(k)}}}^{(D)}] \Big] \in \mathbb{C}^{N \times L_{(k)}} \quad (4)$$

comprises the sampled L1C pilot code sequence with $\mathbf{c}_d[\tau_{\ell_{d_{(k)}}}^{(d)}] \in \mathbb{C}^{N \times 1}$ collecting the periodically repeated pseudo random binary sequences (PRBSs) with time-delay $\tau_{\ell_{d_{(k)}}}^{(d)}$ for each satellite and the respective multipath components. Then, the matrix

$$\tilde{\mathbf{A}} = [\mathbf{a}(\phi_1), \dots, \mathbf{a}(\phi_{L(k)})] \in \mathbb{C}^{M \times L_{(k)}} \quad (5)$$

collects the array responses $\mathbf{a}(\phi_{\ell_{(k)}}) \in \mathbb{C}^{M \times 1}$ with azimuth angle $\phi_{\ell_{(k)}}$ of $\ell_{(k)}$ components at the kth epoch. Moreover, $\mathcal{N}$ is a white Gaussian noise tensor.

The tensor in (1) is composed of three dimensions, the first dimension of size K is related to each epoch, the second dimension of size N is associated with the collected samples in each epoch, and the third dimension of size M corresponds to the spatial diversity of the receive antenna array.

C. POST-CORRELATION DATA MODEL

To separate the $L_{d_{(k)}}$ LOS signals and NLOS multipath components of the dth satellite, the GNSS receiver uses a bank of correlators with respect to each satellite. Thus, the GNSS receiver applies D banks of correlators on the received signal, obtaining D output signals. We define the dth bank of correlators with Q "taps" as

$$\mathbf{Q}_d = \big[\mathbf{c}_d[\tau_1], \dots, \mathbf{c}_d[\tau_Q] \big] \in \mathbb{C}^{N \times Q}, \quad (6)$$
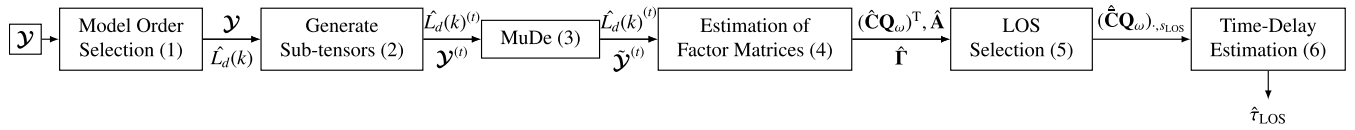
FIGURE 1. Block diagram for the proposed Framework.

with $\tau_1 < \ldots < \tau_Q$ and the qth delayed reference sequence $\mathbf{c}_d[\tau_q]$ corresponding to the qth tap. The thin SVD of $\mathbf{Q}_d$ with

$$\mathbf{Q}_d = \mathbf{U}^{(d)} \Sigma \mathbf{V}^{\mathrm{H}} \quad (7)$$

provides the bank of correlators

$$\mathbf{Q}_\omega^{(d)} = \mathbf{Q}_d (\Sigma \mathbf{V}^{\mathrm{H}})^{-1} \quad (8)$$

which performs cross-correlation (compression) preserving the noise statistics [33]. Therefore, $\mathbf{Q}_\omega^{(d)}$ suppresses other satellites while preserving the noise statistics. When comparing $\mathbf{Q}_\omega^{(d)}$ to the bank of correlators $\mathbf{Q}_d$, we observe that $\mathbf{Q}_d$ provides a sampled cross-correlation function of the bank of correlators with the received LOS component. Thus, according to [10], we can correlate the received signal tensor $\mathcal{X} \in \mathbb{C}^{K \times N \times M}$ with $\mathbf{Q}_\omega^{(d)}$ to separate the dth satellite from all other received satellites and we obtain

$$
\begin{aligned}
\mathcal{Y}^{(d)} \\
&= \mathcal{X} \times_2 (\mathbf{Q}_\omega^{(d)})^{\mathrm{T}} \\
&= \mathcal{I}_{3,L_d} \times_1 \Gamma^{\mathrm{T}} \times_2 (\mathbf{C}\mathbf{Q}_\omega^{(d)})^{\mathrm{T}} \times_3 \mathbf{A} + \mathcal{N} \times_2 (\mathbf{Q}_\omega^{(d)})^{\mathrm{T}} + \mathcal{M} \\
&= \mathcal{I}_{3,L_d} \times_1 \Gamma^{\mathrm{T}} \times_2 (\mathbf{C}\mathbf{Q}_\omega^{(d)})^{\mathrm{T}} \times_3 \mathbf{A} + \mathcal{N}_\omega + \mathcal{M} \\
&\approx \mathcal{I}_{3,L_d} \times_1 \Gamma^{\mathrm{T}} \times_2 (\mathbf{C}\mathbf{Q}_\omega^{(d)})^{\mathrm{T}} \times_3 \mathbf{A} + \mathcal{N}_\omega, \quad (9)
\end{aligned}
$$

where $\mathcal{I}_{3,L_{d(k)}} \in \mathbb{R}^{L_{d(k)} \times L_{d(k)} \times L_{d(k)}}$ is the identity tensor, $\Gamma^{\mathrm{T}} \in \mathbb{C}^{K \times L_{d(k)}}$ collects the complex amplitudes of the $L_{d(k)}$ signal components of satellite d obtained from matrix $\tilde{\Gamma}^{\mathrm{T}}$, $(\mathbf{C}\mathbf{Q}_\omega^{(d)})^{\mathrm{T}} \in \mathbb{R}^{Q \times L_{d(k)}}$ holds the cross-correlation values of the LOS and NLOS components for satellite d, and $\mathbf{A} \in \mathbb{C}^{M \times L_{d(k)}}$ comprises the $L_{d(k)}$ array responses of satellite d excluded from $\tilde{\mathbf{A}}$. In the following we assume that $\mathbf{A}$ does not vary significantly over K epochs. $\mathcal{N}_\omega \in \mathbb{C}^{K \times Q \times M}$ denotes a white Gaussian noise tensor after correlation. The tensor $\mathcal{M}$ is the multiple access interference (cross-correlation) of the other satellites and their respective multipath components. In general, $\mathcal{M}$ is negligible in comparison to other terms, since signals are more or less decorrelated.

IV. PROPOSED FRAMEWORK
As illustrated in Figure 1, the proposed framework can be divided into six steps. In Subsection IV-A we describe block (1). In this step, we receive the post-correlated signal and executes the M-EFT method to estimate the number of multipath components for the dth satellite in dynamic environments. Additionally, in Subsection IV-B, we describe an alternative method for static scenarios, in which we use the RADOI method to estimate the number of multipath components. Next, in Subsection IV-A, we describe block (2) of the framework. In this step, we use the post-correlation

tensor $\mathcal{Y}$ and the estimated model order $L_d(k)$ to generate sub-tensors. In Subsection IV-C, we detail the denoising step in the block (3) by applying the MuDe technique to filter the sub-tensors. Then, block (4), as described in Subsection IV-D, uses the estimated grouped model order and the sub-tensors, filtered by MuDe, to perform the Mode 1 HOSVD SECSI with left-hand matrix (Mode 1 HOSVD SECSI) method to estimate the factor matrices of each sub-tensor. Afterward, as described in Subsection IV-E, block (5) describes how the factor matrices of each sub-tensor are normalized and used to extract the LOS components of all sub-tensors. Finally, as described in Subsection IV-F, we perform TDE of the LOS component of each sub-tensor, as illustrated in the block (6) of the framework given in Figure 1.

A. MODEL ORDER SELECTION FOR DYNAMIC ENVIRONMENTS
To compute the model order applying the Modified Exponential Fitting Test (M-EFT) [24], we use the covariance matrix $\hat{\mathbf{R}}[k]$ obtained from each epoch of the tensor $\mathcal{Y}^{(d)}$ as defined in (9). Therefore, we firstly compute the eigenvalue decomposition (EVD) to obtain

$$\hat{\mathbf{R}}[k] = \frac{1}{Q} \mathcal{Y}^{(d)}[k] \mathcal{Y}^{(d)}[k]^{\mathrm{H}} \quad (10)$$

$$= \mathbf{U}\Lambda\mathbf{U}^{\mathrm{H}} + \mathbf{R}_{qq}[k], \quad (11)$$

where $\hat{\mathbf{R}}[k] \in \mathbb{C}^{M \times M}$ is a Hermitian matrix, $\mathbf{U} = [\mathbf{u}_1 \ \mathbf{u}_2 \ \ldots \ \mathbf{u}_M] \in \mathbb{C}^{M \times M}$ is a unitary matrix containing the eigenvectors, $\Lambda = \mathrm{diag}\{\lambda_1, \ldots, \lambda_M\} \in \mathbb{C}^{M \times M}$ is a diagonal matrix including the the sorted eigenvalues λ_i, such that $\lambda_1 > \lambda_2 > \cdots > \lambda_M$, and the covariance matrix $\mathbf{R}_{qq}[k] \in \mathbb{C}^{M \times M}$ of the bank of correlators. Moreover, we define $\mathbf{U}^{(s)} = [\mathbf{u}_1 \ \mathbf{u}_2 \ \ldots \ \mathbf{u}_P] \in \mathbb{C}^{M \times P}$ as the truncated matrix composed of P eigenvectors of $\mathbf{U}$ corresponding to the P largest eigenvalues of Λ. Therefore, in case that $P = L_{d(k)}(k)$, the dominant eigenvectors $\mathbf{U}^{(s)} \in \mathbb{C}^{M \times L_{d(k)}(k)}$ and the column space of the steering matrix $\mathbf{A}$ span the same subspace.

Furthermore, the M-EFT can adopt an exponential profile to approximate the Wishart profile of the noise eigenvalues and consequently enabling their prediction. The M-EFT estimates the model order by computing the distance from λ_{M-P}, calculated from the measurements to the predicted eigenvalue $\hat{\lambda}_{M-P}$, where P is a possible number of noise eigenvalues. Furthermore, the M-EFT method computes the threshold coefficients η_P, and then estimates the model order. Since M, Q, and the probability of false alarm P_{fa}, do not vary, η_P is computed previously and stored. To compute the M-EFT we refer to [24], [34].

(a) $K = 5, L_{d_{1(k)}}^{\hat{}} = 2$

(b) $K = 3, L_{d_{2(k)}}^{\hat{}} = 3$

FIGURE 2. Sub-tensors obtained after grouping the epochs with same estimated model order.

Then, once we have the estimated model order $\hat{L}_{d_{(k)}}(k)$ for each epoch, we group the epochs with the same estimated model order, as illustrated in Figure 2(a) and 2(b). Moreover, we create a vector that contains the grouped model order $\hat{L}_{d_{(k)}}(k)^{(t)}$ with respect to the epochs and for $t = 1, \ldots, T$ sub-tensors. Therefore, we create $\tilde{\mathcal{Y}}^{(t)}$ sub-tensors which will be used to perform TDE. For instance, if we estimate three different model orders $\hat{L}_{d_1}(k) = 2$ and $\hat{L}_{d_2}(k) = 3$ we concatenate the epochs with the same model order to create a new tensor. Afterwards, we can use the sub-tensors to perform TDE.

B. MODEL ORDER SELECTION FOR STATIC ENVIRONMENTS

In order to decompose the tensor $\mathcal{Y}^{(d)}$ into factor matrices for TDE, first, the number of multipath components of the dth satellite $L_{d_{(k)}}$ have to be estimated. To perform MOS in static environments we propose to apply RADOI [26] for which the covariance matrix $\hat{R}_{yy}$ obtained from the third-mode unfolding of tensor $[\mathcal{Y}^{(d)}]_{(3)}$ as defined in (9) is used to compute an EVD. Thus, we obtain

$$\hat{R}_{yy} = \frac{1}{KQ}[\mathcal{Y}^{(d)}]_{(3)}[\mathcal{Y}^{(d)}]_{(3)}^{\text{H}} \qquad (12)$$

$$= \tilde{U}\tilde{\Lambda}\tilde{U}^{\text{H}} + R_{qq}^{\text{R}}, \qquad (13)$$

where $\hat{R}_{yy} \in \mathbb{C}^{M \times M}$ is a Hermitian matrix, $\tilde{u} = [\tilde{u}_1 \, \tilde{u}_2 \, \ldots \, \tilde{u}_M] \in \mathbb{C}^{M \times M}$ is an unitary matrix containing the eigenvectors, $\tilde{\Lambda} = \text{diag}\{\tilde{\lambda}_1, \ldots, \tilde{\lambda}_M\} \in \mathbb{C}^{M \times M}$ is a diagonal matrix collecting the sorted eigenvalues $\tilde{\lambda}_i$, such that $\tilde{\lambda}_1 > \tilde{\lambda}_2 > \cdots > \tilde{\lambda}_M$, and the covariance matrix $R_{qq}^{\text{R}} \in \mathbb{C}^{M \times M}$ of the bank of correlators. Moreover, we define $\tilde{U}^{(s)} = [\tilde{u}_1 \, \tilde{u}_2 \, \ldots \, \tilde{u}_P] \in \mathbb{C}^{M \times P}$ as the truncated matrix composed of P eigenvectors of $\tilde{U}$ corresponding to the P largest eigenvalues of $\tilde{\Lambda}$. Therefore, as discussed above for the EFT, in case that $P = L_{d_{(k)}}$, the dominant eigenvectors $U^{(s)R} \in \mathbb{C}^{M \times L_{d_{(k)}}}$ and the column space of the steering matrix A span the same subspace.

C. TENSOR-BASED MULTIPLE DENOISING

Since TDE performance is sensitive to signal-to-noise ratio (SNR) and degrades in noisy scenarios, we include a denoising step. Therefore, we propose to use the MuDe approach [31], which is a pre-processing technique to denoise tensor-like data. MuDe combines the principle of Spatial Smoothing (SPS) [12] with successive SVD-based low-rank

approximations of the output signals for sub-arrays of varying size in each spatial dimension of the obtained signal tensor and, then, rebuilds the the different sub-arrays into a tensor.

D. ESTIMATION OF FACTOR MATRICES

Originally, the state-of-the-art SECSI method [21] offers a trade-off between performance and reliability. The authors in [21] prove that for a 3-way tensor, one can construct six distinct diagonalization problems by computing the slices of the core tensor. Then, one can use each core tensor to compute the right-hand and left-hand matrices of each slice. Following the solution of the six distinct diagonalization problems, the authors in [21] propose to analyze the estimates and, then, select the estimate with the lowest error. However, to reduce processing time, [20] proposes to utilize only the right-hand matrix obtained from the first-mode slice of the core tensor. Moreover, in [20] it was shown that the SECSI method combined with HOSVD (HOSVD SECSI) introduced in [21] presents a higher complexity than the CPD-GEVD. However, despite the higher complexity of the HOSVD SECSI, this method shows better performance in scenarios with highly correlated signals. Consequently, the HOSVD SECSI method is more reliable in more demanding scenarios. However, based on simulations, we show that, by applying different tensor modes, we can also achieve better performance in dynamic situations.

Since we create a sub-tensor for the tensor epochs with the same model order, in some situations, we obtain a model order greater than the number of epochs in a given sub-tensor. Since the method used in [20] is no longer suitable for a dynamic scenario, we propose to apply a different tensor mode to perform factor matrix estimation. Hence, in several simulations, the left-hand matrix obtained from the third-mode slice of the core tensor (Mode 1 HOSVD SECSI) $\mathcal{S}^{(d)^{(t)}}$ proved to be a suitable alternative. Finally, to compute the Mode 1 HOSVD SECSI we firstly compute the HOSVD low-rank approximation of the sub-tensors $\mathcal{Y}^{(d)^{(t)}}$ obtained from grouping the tensor $\mathcal{Y}^{(d)}$ epochs according to their model order.

$$\mathcal{Y}^{(d)^{(t)}} \approx \mathcal{S}^{(d)^{(t)}} \times_1 U_1^{(d)^{(t)}} \times_1 U_2^{(d)^{(t)}} \times_3 U_3^{(d)^{(t)}}, \qquad (14)$$

where the superscript $^{(t)}$ indicates the tth sub-tensor, $U_1^{(d)^{(t)}} \in \mathbb{C}^{K \times L_{d_{(k)}}}$, $U_2^{(d)^{(t)}} \in \mathbb{C}^{Q \times L_{d_{(k)}}}$, and $U_3^{(d)^{(t)}} \in \mathbb{C}^{M \times L_{d_{(k)}}}$, are the truncated singular matrices related to the tth sub-tensor. Moreover, to compute the singular matrices and the core tensor, the SVD is derived for each of the unfolding of the tensor for each dimension. Thus, we can write

$$\left[\mathcal{Y}^{(d)}\right]_{(1)}^{(t)} = U_1^{(d)^{(t)}} S_1^{(d)^{(t)}} V_1^{\text{H}(d)^{(t)}}, \qquad (15)$$

$$\left[\mathcal{Y}^{(d)}\right]_{(2)}^{(t)} = U_2^{(d)^{(t)}} S_2^{(d)^{(t)}} V_2^{\text{H}(d)^{(t)}}, \qquad (16)$$

$$\left[\mathcal{Y}^{(d)}\right]_{(3)}^{(t)} = U_3^{(d)^{(t)}} S_3^{(d)^{(t)}} V_3^{\text{H}(d)^{(t)}}, \qquad (17)$$

where $\mathbf{U}_i^{(d)^{(t)}}$, $\mathbf{S}_i^{(d)^{(t)}}$, and $\mathbf{V}_i^{\mathrm{H}(d)^{(t)}}$ are the left singular vector matrix, singular value matrix, and right singular vector matrix for the *i*th dimension, respectively. Consider that the left singular vector matrices can be sequentially computed as follows:

$$\left[\mathcal{Y}^{(d)}\right]_{(1)}^{(t)} = \mathbf{U}_1^{(d)^{(t)}}\mathbf{S}_1^{(d)^{(t)}}\mathbf{V}_1^{\mathrm{H}(t)}, \qquad (18)$$

$$\left[\mathcal{Y}^{(d)^{(t)}} \times_1 \mathbf{U}_1^{\mathrm{H}(t)}\right]_{(2)} = \mathbf{U}_2^{(d)^{(t)}}\mathbf{S}_2^{(d)^{(t)}}\mathbf{V}_2^{\mathrm{H}(t)}, \qquad (19)$$

$$\left[\mathcal{Y}^{(d)^{(t)}} \times_1 \mathbf{U}_1^{\mathrm{H}(t)} \times_2 \mathbf{U}_2^{\mathrm{H}(t)}\right]_{(3)} = \mathbf{U}_3^{(d)^{(t)}}\mathbf{S}_3^{(d)^{(t)}}\mathbf{V}_3^{\mathrm{H}(d)^{(t)}}. \qquad (20)$$

Next, let us consider the first-mode unfolding of $\mathcal{Y}^{(d)}$ and use the representation in (9) and (14), then, we obtain

$$\mathbf{U}_1^{(d)^{(t)}}[\mathcal{S}]_{(1)}^{(t)}(\mathbf{U}_2^{(d)^{(t)}} \otimes \mathbf{U}_3^{(d)^{(t)}})^{\mathrm{T}}$$
$$= \Gamma^{\mathrm{T}(t)}[\mathcal{I}_{3,\mathrm{L}}]_{(1)}^{(t)}((\mathbf{CQ}_\omega^{(d)^{(t)}})^{\mathrm{T}} \otimes \mathbf{A}^{(t)})^{\mathrm{T}}. \qquad (21)$$

Hence, the subspace spanned by the columns of $\mathbf{U}_1^{(d)^{(t)}}$, $\mathbf{U}_2^{(d)^{(t)}}$, and $\mathbf{U}_3^{(d)^{(t)}}$ and the subspace spanned by the columns of $\Gamma^{(\mathbf{t})^{\mathrm{T}}}$, $(\mathbf{CQ}_\omega^{(d)^{(t)}})^{\mathrm{T}}$, and $\mathbf{A}^{(t)}$ are identical. Consequently, there exists a set of non-singular transform matrices $\mathbf{T}_1^{(t)} \in \mathbb{C}^{L_{d(k)} \times L_{d(k)}}$, $\mathbf{T}_2^{(t)} \in \mathbb{C}^{L_{d(k)} \times L_{d(k)}}$, and $\mathbf{T}_3^{(t)} \in \mathbb{C}^{L_{d(k)} \times L_{d(k)}}$ which represent the loading matrices of the CPD of the core tensor of the HOSVD given in (14). Thus, the tensor $\mathcal{S}$ can be represented as

$$\mathcal{S}^{(d)^{(t)}} = \mathcal{I}_{3,L_{d(k)}}^{(t)} \times_1 \mathbf{T}_1^{(t)} \times_2 \mathbf{T}_2^{(t)} \times_3 \mathbf{T}_3^{(t)}. \qquad (22)$$

The transform matrices $\mathbf{T}_1^{(t)} \in \mathbb{C}^{L_{d(k)} \times L_{d(k)}}$, $\mathbf{T}_2^{(t)} \in \mathbb{C}^{L_{d(k)} \times L_{d(k)}}$, and $\mathbf{T}_3^{(t)} \in \mathbb{C}^{L_{d(k)} \times L_{d(k)}}$ represent the loading matrices of the CPD of the core tensor $\mathcal{S}^{(d)^{(t)}} \in \mathbb{C}^{L_{d(k)} \times L_{d(k)} \times L_{d(k)}}$ in (22). In theory, the CPD can be directly applied to $\mathcal{Y}^{(d)}$, to extract the factor matrices. However, as demonstrated in [10], by directly computing the factor matrices using Alternating Least Squares (ALS), there are convergence problems, resulting into poor performance in terms of TDE. Therefore, to perform the CPD, it is sufficient to compute the loading matrices $\mathbf{T}_1^{(t)}$, $\mathbf{T}_2^{(t)}$, and $\mathbf{T}_3^{(t)}$, to obtain the factor matrices

$$\mathbf{U}_1^{(d)^{(t)}}\mathbf{T}_1^{(t)} = \Gamma^{(\mathbf{t})^{\mathrm{T}}}, \qquad (23)$$

$$\mathbf{U}_2^{(d)^{(t)}}\mathbf{T}_2^{(t)} = \left(\mathbf{CQ}_\omega^{(d)^{(t)}}\right)^{\mathrm{T}}, \qquad (24)$$

$$\mathbf{U}_3^{(d)^{(t)}}\mathbf{T}_3^{(t)} = \mathbf{A}^{(t)}. \qquad (25)$$

As a consequence of the symmetry of the SECSI problem, we can build 6 Simultaneous Matrix Diagonalization (SMD) problems for a three-way model [21]. However, as shown by [20], without loss of generality, we can only use one mode of the compressed core tensor $\mathcal{S}^{(d)^{(t)}}$ to compute the right-hand and left-hand matrices utilized in the SMD step described in [21]. In [20], the authors show that the SECSI third-mode, of a given compressed core tensor, in the GNSS case, yields the best estimation performance in static scenarios. However, after performing several numerical simulations,

we now select the left-hand matrix of the first mode of the compressed core tensor $\mathcal{S}^{(d)^{(t)}}$. Therefore, the *i*th slice of the first-mode of tensor $\mathcal{S}^{(d)^{(t)}}$ is selected to compute the left-hand matrix

$$\mathbf{S}_{1,i}^{(t)} = \left[\left(\mathcal{S}^{(d)^{(t)}} \times_1 \mathbf{U}_1^{(d)^{(t)}}\right) \times_1 \mathbf{e}_i^{\mathrm{T}}\right]$$
$$= \mathbf{T}_2^{(t)} \mathrm{diag}\{\Gamma^{(\mathbf{t})^{\mathrm{H}}}_{\cdot,i}\}\mathbf{T}_3^{(t)^{\mathrm{T}}}, \qquad (26)$$

where $\mathbf{e}_i^{\mathrm{T}}$ is a vector with all zeros except in the *i*th position. Next, we select the slice of the tensor $\mathcal{S}^{(d)^{(t)}}$ with the smallest condition number

$$\mathbf{S}_{1,p}^{(d)^{(t)}} = \mathbf{T}_2^{(d)^{(t)}} \mathrm{diag}\{\Gamma^{(d)^{(t)\mathrm{H}}}_{\cdot,p}\}(\mathbf{T}_3^{(d)^{(t)}})^{\mathrm{T}}, \qquad (27)$$

where *p* is an arbitrary index between one and the total number of slices to be diagonalized and defines the slice of the tensor $\mathcal{S}^t$ with the smallest condition number

$$p = \arg\min_i \mathrm{cond}\{\mathbf{S}_{1,i}^{(d)^{(t)}}\}, \qquad (28)$$

where $\mathrm{cond}\{\cdot\}$ computes the condition number of a matrix. The smaller the condition number of a matrix, the more stable is its inversion. Furthermore, we obtain the left-hand matrices $\mathbf{S}_{1,i}^{(t),\mathrm{lhs}}$ by multiplying $\mathbf{S}_{1,i}$ by $\mathbf{S}_{1,p}$ on the left-hand side

$$\mathbf{S}_{1,i}^{(d),\mathrm{lhs}^{(t)}} = \left(\mathbf{S}_{1,p}^{(d)^{(t)}-1}\mathbf{S}_{1,i}^{(d)^{(t)}}\right)^{\mathrm{T}}$$
$$= \mathbf{T}_3^{(d)^{(t)}}\Gamma^{(d)^{(t)\mathrm{H}}}\mathbf{T}_3^{(d)^{(t)}-1}. \qquad (29)$$

Since *p* is fixed, we can *i* in (29) obtaining $N-1$ equations, since $i \neq p$. Our goal is to find $\hat{\mathbf{T}}_3^{(d)^{(t)}}$ that simultaneously diagonalizes the $N-1$ equations. We refer here to the techniques in [35] and [36].

Since in the noiseless case, according to (9), the third-mode unfolding exposes the factor matrix $\mathbf{A}^{(t)}$, we can write

$$[\mathcal{Y}^{(d)^{(t)}}]_{(3)}^{\mathrm{T}} = \left[\Gamma^{(t)} \diamond \left(\mathbf{CQ}_\omega^{(d)}\right)^{(t)}\right]\mathbf{A}^{(t)}. \qquad (30)$$

Using $\mathbf{U}_3^{(d)^{(t)}}$ from (14) and $\hat{\mathbf{T}}_3^{(t)}$ from the diagonalization step we obtain

$$\mathbf{U}_3^{(d)^{(t)}}\hat{\mathbf{T}}_3^{(t)} = \hat{\mathbf{A}}^{(t)}. \qquad (31)$$

Afterwards, we multiply (30) by the pseudo-inverse of the estimated $\hat{\mathbf{A}}^{(t)}$ from the left-hand side to obtain

$$\mathbf{F}^{(t)} = [\mathcal{Y}^{(d)^{(t)}}]_{(3)}^{\mathrm{T}}(\hat{\mathbf{A}}^{(t)})^{+\mathrm{T}}$$
$$= \left[\Gamma^{(t)} \diamond \left(\mathbf{CQ}_\omega^{(d)}\right)^{(t)}\right]\mathbf{A}^{(t)}(\hat{\mathbf{A}}^{(t)})^{+\mathrm{T}}$$
$$\approx \left[\Gamma^{(t)} \diamond \left(\mathbf{CQ}_\omega^{(d)}\right)^{(t)}\right] \in \mathbb{C}^{KM \times L_{d(k)}}. \qquad (32)$$

Then, the factor matrices $(\mathbf{CQ}_\omega^{(d)^{(t)}})^{\mathrm{T}}$ and $\Gamma^{(t)}$ can be estimated from (32) by applying the Least Squares Khatri-Rao Factorization (LSKRF) [37].

E. LOS SELECTION

Subsequently, to estimating all the parameters of the received signal, we need to separate the LOS and NLOS signal parameters. In this subsection, we describe the fifth element of the framework. This element performs the LOS selection based on the estimated factor matrices. Therefore, as described in [20], to perform the LOS selection the estimated factor matrices $(\hat{\mathbf{C}}\mathbf{Q}_\omega^{(d)}))^{(t)\mathrm{T}}$, $\hat{\mathbf{A}}^{(t)}$, and $\hat{\Gamma}^{(t)}$ are normalized to unit norm for the $\ell_d^{(t)}$th component and can be given as

$$(\hat{\hat{\mathbf{C}}\mathbf{Q}}_\omega^{(d)})_{\cdot,\ell_d^{(t)}}^{(t)\mathrm{T}} = (\hat{\mathbf{C}}\mathbf{Q}_\omega^{(d)})_{\cdot,\ell_d^{(t)}}^{(t)\mathrm{T}}/||(\hat{\mathbf{C}}\mathbf{Q}_\omega^{(d)})_{\cdot,\ell_d^{(t)}}^{(t)\mathrm{T}}||_F, \quad (33)$$

$$\hat{\hat{\mathbf{A}}}_{\cdot,\ell_d^{(t)}}^{(t)} = \hat{\mathbf{A}}_{\cdot,\ell_d^{(t)}}^{(t)}/||\hat{\mathbf{A}}_{\cdot,\ell_d^{(t)}}^{(t)}||_F, \quad (34)$$

$$\hat{\hat{\Gamma}}_{\cdot,\ell_d^{(t)}}^{(t)} = \hat{\Gamma}_{\cdot,\ell_d^{(t)}}^{(t)}/||\hat{\Gamma}_{\cdot,\ell_d^{(t)}}^{(t)}||_F. \quad (35)$$

Next, with the normalized factor matrices, we construct the tensor $\mathcal{G}_{\ell_d^{(t)}}^{(t)}$ for the $\ell_d^{(t)}$th normalized component of the estimated factor matrices

$$\mathcal{G}_{\ell_d^{(t)}}^{(t)} = \hat{\hat{\Gamma}}_{\cdot,\ell_d^{(t)}}^{(t)} \circ (\hat{\hat{\mathbf{C}}\mathbf{Q}}_\omega^{(d)})_{\cdot,\ell_d^{(t)}}^{(t)\mathrm{T}} \circ \hat{\hat{\mathbf{A}}}_{\cdot,\ell_d^{(t)}}^{(t)}, \quad (36)$$

where $\mathcal{G}_{\ell_d^{(t)}}^{(t)} \in \mathbb{C}^{K \times Q \times M}$. Then, we store the tensor $\mathcal{G}_{\ell_d^{(t)}}^{(t)}$ corresponding to the $\ell_d^{(t)}$th component in a matrix

$$\mathbf{G}_{\cdot,\ell_d^{(t)}}^{(t)} = \mathrm{vec}\{\mathcal{G}_{\ell_d^{(t)}}^{(t)}\}, \quad (37)$$

where $\mathbf{G}^{(t)} \in \mathbb{C}^{KQM \times L_d}$, and $\mathrm{vec}\{\mathcal{G}_{\ell_d^{(t)}}^{(t)}\}$ vectorize the tensor $\mathcal{G}_{\ell_d^{(t)}}^{(t)}$. Thus, we can compute the tensor amplitudes by multiplying the pseudoinverse of $\mathbf{G}^{(t)}$ by the $\mathrm{vec}\{\tilde{\mathcal{Y}}^{(d)^{(t)}}\}$ and we obtain

$$\boldsymbol{\gamma}^{(t)} = \mathbf{G}^{(t)+} \mathrm{vec}\{\tilde{\mathcal{Y}}^{(d)^{(t)}}\}. \quad (38)$$

Assuming that the received signal component with the largest power corresponds to the LOS signal, we select the respective column of the estimated $(\hat{\hat{\mathbf{C}}\mathbf{Q}}_\omega^{(d)})^{(t)\mathrm{T}}$ with

$$\hat{\ell}_d^{(t)} = \arg \max_{\ell_d^{(t)}=1,\ldots,L_d^{(t)}} |\boldsymbol{\gamma}_{\ell_d^{(t)},\cdot}^{(t)}|^2. \quad (39)$$

F. TIME-DELAY ESTIMATION (TDE)

Once we have selected the LOS component, in this Subsection, we describe the sixth element of the framework by describing the TDE process. Therefore, we use the s_{LOS} from the third element to select the LOS component from the estimated $(\hat{\hat{\mathbf{C}}\mathbf{Q}}_\omega^{(d)})^{(t)\mathrm{T}}$ and multiply it by $\Sigma\mathbf{V}^{\mathrm{H}}$ from the thin SVD of $\mathbf{Q}_d$

$$\mathbf{q} = \left[(\hat{\hat{\mathbf{C}}\mathbf{Q}}_\omega^{(d)})_{\cdot,s_{\mathrm{LOS}}}^{(t)\mathrm{T}} \Sigma\mathbf{V}^{\mathrm{H}}\right]^{\mathrm{T}}. \quad (40)$$

where $\mathbf{q}$ contains the cross-correlation values at each tap of the correlator bank. Then, as shown in [10], [14], [15], [20], [38], [39], the resulting vector $\mathbf{q}$ is interpolated using a simple cubic spline interpolation. Thus, by using the resulting interpolated vector, we can derive the cost function $F(\kappa)$ [20],

which is the cross-correlation function with the received LOS signal. Finally, we use this cost function to estimate the time-delay of the LOS signal by solving

$$\hat{\tau}^{(d)^{(t)}}_{\mathrm{LOS}} = \arg \max_\kappa F(\kappa). \quad (41)$$

V. RESULTS

Following [16], we first consider a static scenario that consists of a left centro-hermitian uniform linear array (ULA) with $M = 8$ elements and half-wavelength $\Delta = \lambda/2$ spacing. The L1C pilot channel is transmitted by the satellites with $PRS = 3, 4, 17$ with a carrier frequency $f_s = 1575.42$ MHz. The simulations consider a GPS L1C pilot signal with a period $t_{3rd} = 10$ ms and with a bandwidth $B = 12.276$ MHz. The L1C pilot code samples are collected every kth epoch during $K = 30$ epochs with each epoch having a duration of 10 ms [16] and with a sampling frequency $f = 2B$ MHz. Therefore, $N = 245520$ samples are collected for the L1C pilot code per epoch. The carrier-to-noise ratio is $C/N_0 = 48$ dB-Hz, resulting in a pre-correlation signal-to-noise ratio $SNR_{\mathrm{pre}} = C/N_0 - 10\log_{10}(2B) \approx -25.10$ dB for GPS3. Given the processing gain $G = 10\log_{10}(Bt) \approx 50.9$ dB for GPS3. Hence, the post-correlation signal-to-noise ratio $SNR_{\mathrm{post}} = SNR_{\mathrm{pre}} + G \approx 25$ dB. Moreover, the signal-to-multipath ratio $SMR_1 = 5$ dB for $L_d = 2$. In case $L_d = 3$ the $SMR_1 = 5$ dB for the first NLOS signal, and a $SMR_2 = 10$ dB for the second NLOS signal. Besides the simulation considering exact knowledge of the array response (perfect array), we added errors in the antenna array geometry to distort the real array response with respect to the known response by displacing the antennas in x and y positions according to a normal distribution $\sim\mathcal{N}(0, \sigma^2)$. The standard deviation is computed in terms of the probability $p = \mathrm{P}(e > \lambda/2)$, where the error exceeds a half wavelength. We fix the relative time-delay $\Delta\tau$ at $0.5T_c$ while varying the error probability p from 10^{-6} to 10^{-1}. Moreover, we consider a probability of false alarm $P_{\mathrm{fa}} = 10^{-3}$.

Additionally, we performed simulations considering a dynamic scenario with one satellite with $PRBS = 17$. In this dynamic scenario, we vary the DoA of the LOS component for each epoch and the number of LOS and NLOS components within the tensor $\mathcal{Y}$. We define a DoA difference between epochs of $2°$. Moreover, we define the first 15 epochs have $L_d = 5$ while the last fifteen collected epochs have $L_d = 6$. Since we consider a dynamic scenario, we target a lower probability of false alarm $P_{\mathrm{fa}} = 10^{-6}$.

Since [20] showed that simulations potentially have outliers in case the signals are strongly correlated, we, therefore, performed 1000 Monte Carlo (MC) simulations to compare all approaches in terms of the Root Median-Squared Error (RMDSE) of the time-delay of the LOS component. The TDE performance of the proposed tensor-based methods is compared to the TDE performance in the case $\mathbf{A}$ and Γ are considered known, which can be considered as a lower bound for TDE performance for the proposed methods.

TABLE 1. Probability of Detection for MOS with $M = 8$ antennas. In both cases code samples are collected during $K = 30$ epochs, and $N = 245520$.

	PoD $d = 1$ and $L_d = 3$	PoD $d = 3$ and $L_d = 3$
EFT	99%	0%
M-EFT	99%	0%
MDL	99%	0%
AIC	85%	0%
R-D AIC	99%	0%
R-D MDL	99%	0%
R-D EFT	99%	1%
RADOI	100%	99%
ESTER	100%	99%

A. PROBABILITY OF DETECTION CONSIDERING A STATIC SCENARIO

In this section, we present the probability of detection (PoD) for simulations considering an array of antennas for which the array response is known. We compute the PoD for a relative delay $\Delta\tau = 0.5T_c$. In TABLE 1, we show the PoD for static scenarios with $d = 1$ satellite with $L_d = 3$ components and $d = 3$ satellites with $L_d = 3$ components. Note that, in the simplest scenario, $d = 1$ and $L_d = 3$, only AIC presents a PoD below 99%. However, observe that if we add more satellites to the simulations, the EFT, AIC, and MDL-based methods do not correctly estimate the model order. However, note that both RADOI and ESTER methods have a consistent performance achieving the same PoD for all simulations.

TABLE 2. Probability of detection for MOS methods with an imperfect array with $M = 8$ antennas. In both cases code samples are collected during $K = 30$ epochs with $N = 245520$.

	PoD $d = 1$ and $L_d = 3$	PoD $d = 3$ and $L_d = 3$
EFT	99%	23%
M-EFT	99%	30%
MDL	99%	50%
AIC	85%	10%
R-D AIC	99%	0%
R-D MDL	99%	0%
R-D EFT	99%	18%
RADOI	100%	99%
ESTER	17%	5%

1) PoD CONSIDERING AN ARRAY WITH ERRORS AND A STATIC SCENARIO

In this section we consider an antenna array with errors in its array response model (imperfect array) with $d = 1$ and $L_d = 2$, $d = 1$ and $L_d = 3$ impinging signals, and a fixed relative time-delay $\Delta\tau = 0.5T_c$. In TABLE 2, we show the PoD for the MOS methods for $d = 1$ satellite with $L_d = 3$ impinging signals and $d = 3$ satellite with $L_d = 3$ impinging signals. Note that the ESTER method shows an inferior performance when we add a second NLOS component to the simulation. Observe that in case the array response model of the antenna array includes errors (e.g. the antenna elements of the array experienced displacement errors), the eigenvalue-based methods EFT, M-EFT, MDL, R-D AIC, R-D MDL, R-D EFET, and RADOI, are insensitive to these errors in the array

response model. However, since the ESTER method assumes the matrix **A** has a Vandermonde structure, errors in the array response model cause that the matrix **A** has a different structure than Vandermonde. Therefore, the ESTER shows to be sensitive to array imperfections. Moreover, we can observe that RADOI is the most accurate MOS method in a static environment.

B. TDE CONSIDERING A STATIC SCENARIO

In this section, we present simulation results of the various methods for the GPS3 L1C signal. We assess the case $L_d = 3$ and $d = 3$. Additionally, preceding the time-delay estimation, we apply the RADOI method since other matrix and tensor-based methods, do not provide reliable estimates.
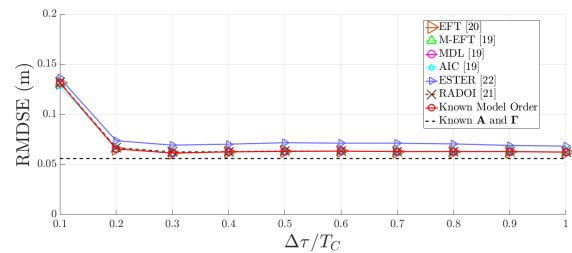

FIGURE 3. MOS techniques and proposed Mode 1 HOSVD SECSI with left-hand matrix method simulation with $M = 8$ antennas. In both cases code samples are collected during $K = 30$ epochs, $N = 245520$, and $L_d = 3$ and $d = 3$.

In Figure 3 we show the TDE error for matrix-based MOS methods in a static scenario. Note that the results obtained by RADOI present similar estimates to the known model order case. Moreover, in the case signals are weakly correlated, e. g., $\Delta\tau > 0.2Tc$, the RADOI method provides precise model order estimates. Note that in a static scenario with constant model order, the MOS accuracy seems irrelevant since the TDE performance is similar. The larger power of the LOS component after signal correlation explains the similar TDE. However, the Mode 1 HOSVD SECSI shows higher estimation errors when combined with the AIC since AIC provides an estimated model order of $L_d > 5$. Thus, to keep the TDE error as low as possible, it is essential to use a reliable MOS scheme.

C. PROBABILITY OF DETECTION CONSIDERING A DYNAMIC SCENARIO

In this section, we present the PoD computed considering a dynamic scenario and a perfectly aligned array of antennas with no errors in the array response model. In dynamic scenarios, the number of LOS and NLOS components within the tensor $\mathcal{Y}^{(d)}$ are changing. When applying matrix-based MOS methods, we performed the MOS for each epoch and individually computed the PoD. Moreover, in a dynamic scenario, we use the pre-processing methods FBA, SPS, and their combinations to attempt to improve the model order estimation accuracy in case of highly correlated signal components.

In Figure 4 we show the PoD for the M-EFT method for $\Delta\tau = 0.1 T_c$ and $K = 30$. Note that the M-EFT method
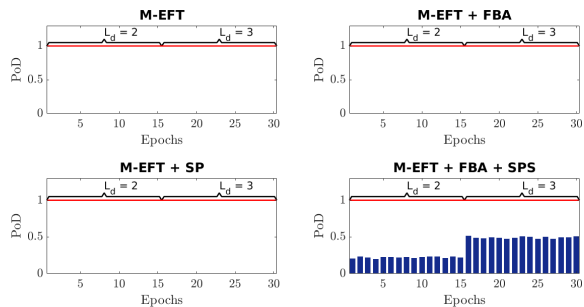
FIGURE 4. PoD of EFT for $\Delta\tau = 0.1\ T_c$ in a dynamic scenario with an perfect array with $M = 8$ antennas. Code samples are collected during $K = 30$ epochs with $N = 245520$.
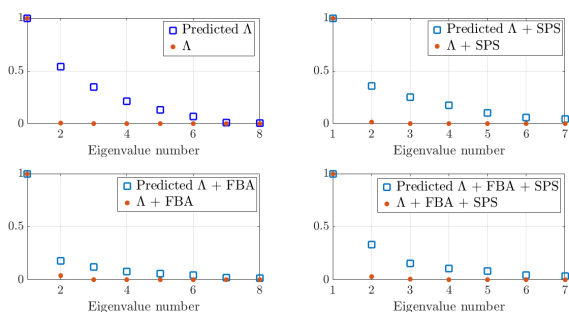

FIGURE 5. M eigenvalues and M predicted eigenvalues at $\Delta\tau = 0.1\ T_c$ of the first epoch of tensor $\mathcal{Y}^{(d)}$ and $L_d = 5$.

fails to estimate the model order but applying FBA and SPS, M-EFT shows a PoD above 20% when $L_d = 5$ and above 50% when $L_d = 6$.

In Figure 5, we show the M eigenvalues and the M predicted eigenvalues, at $\Delta\tau = 0.1\ T_c$. The eigenvalues are normalized with respect to the strongest eigenvalue (LOS eigenvalue). In Figure 5 one can observe, that FBA and SPS add some gain to the NLOS components. However, since the NLOS components' power is too small, we obtain low NLOS eigenvalues. Note that the 3rd, 4th, and 5th eigenvalues are as weak as the noise eigenvalues, i.e., 6th, 7th, and 8th eigenvalues. Although the eigenvalues are weak, note that, when we combine the FBA and SPS, we obtain a significant gain to allow a more accurate MOS.

Therefore, the AIC, ESTER, and RADOI methods are not suitable to perform MOS for GPS3 signals in dynamic environments. MDL, EFT, and M-EFT also show poor performance. However, when applying the pre-processing methods FBA and SPS, we can improve the MOS performance. Mainly, we can achieve better results when combining these pre-processing methods with the MDL, EFT, and M-EFT methods. Since the matrix-based MOS methods use slices of the full tensor, the additional simulations showed that the PoD remains constant as we increase the number of collected epochs. Moreover, we performed simulations with $\Delta\tau > 0.1T_c$, and we observed that the PoD increases as we increased $\Delta\tau$. Therefore, in case the LOS and NLOS components are separated adequately in time, the MOS methods will show better performance, as the different signal components are less correlated in time.

D. TDE CONSIDERING A DYNAMIC SCENARIO

In this section, we present the TDE performance for simulations considering a dynamic scenario and a perfectly aligned array of antennas with no errors in the array response model.

Since the matrix-based AIC, ESTER, and RADOI methods showed poor performance in a dynamic scenario, we only used the matrix-based MDL+FBA+SPS, EFT+FBA+SPS, and EFT+FBA+SPS methods. Additionally, we performed simulations considering the model order to be known for each epoch. Thus, we could divide the main tensor into new sub-tensors and then perform TDE for each sub-tensor. Additionally, we present results for the Tensor-based Eigenfilter. Differently from the CPD-based methods, the Tensor-based Eigenfilter does not require an estimate of the model order to perform TDE of the LOS component. Therefore, the Tensor-based Eigenfilter might be a suitable alternative in a dynamic scenario. Finally, the CPD-GEVD and the HOSVD SECSI methods are not suitable to be combined with the approach in which we create sub-tensors to perform TDE. Since both methods use the dimension of epochs, e.g., dimension K, of the tensors to perform factor matrix estimation in some scenarios with $\hat{L}_d > K$ the tensor factorization becomes impossible.
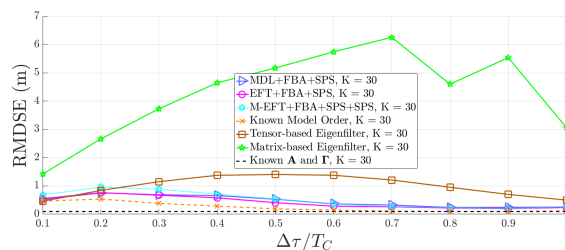

FIGURE 6. Results of MOS techniques and the proposed Mode 1 HOSVD SECSI with left-hand matrix method and $M = 8$ antennas. In both cases code samples are collected during $K = 30$ epochs, $N = 245520$, and $L_d = 5$ and $L_d = 6$.

Since the HOSVD SECSI method is not suitable for the sub-tensor approach, we exploit the tensor dimensions that could be used to perform tensor factorization. Thus, we, alternatively, use the proposed Mode 1 HOSVD SECSI with the left-hand slices of the core tensor. In contrast to the HOSVD SECSI, the proposed Mode 1 HOSVD SECSI with left-hand slices of the core tensor uses the antenna dimension, i.e., the third dimension of the tensor $\mathcal{Y}^{(d)}$, to perform tensor factorization while the HOSVD SECSI uses the epochs dimension, i.e., the first dimension of the tensor $\mathcal{Y}^{(d)}$. In Figure 6 we show simulation results for the proposed Mode 1 HOSVD SECSI with left-hand matrix slices with $K = 30$. As previously described, we use the matrix-based MOS methods to estimate the model order for each epoch, then we group the epochs with the same model order and create sub-tensors. Therefore, since the sub-tensor approach is a solution that aims to create pseudo-static scenarios, we show that the HOSVD SECSI variant is suitable to perform tensor factorization and TDE when applying the sub-tensor approach.
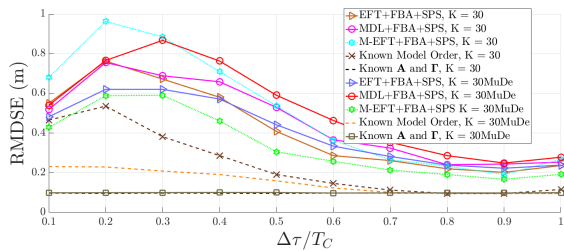
FIGURE 7. MuDe method, MOS techniques and proposed Mode 1 HOSVD SECSI with left-hand matrix method and $M = 8$ antennas. In both cases code samples are collected during $K = 30$ epochs, $N = 245520$, and $L_d = 5$ and $L_d = 6$.

E. TDE CONSIDERING A DYNAMIC SCENARIO WITH MuDe

In this section, we discuss TDE considering a dynamic scenario, a perfectly aligned array of antennas (no errors in the array response model), and the MuDe technique. When applying matrix-based MOS methods, we again grouped the epochs with the same estimated model order, as described previously. The MuDe technique cannot be applied to the Tensor-based Eigenfilter and a simpler matrix-based eigenfilter. For simulations with $\Delta\phi = 10°$ most MOS techniques failed to correctly estimate $L_d^{(t)}$ by either overestimating or not being capable of determining the model order. However, when $\Delta\phi = 10°$ we could estimate $L_d^{(t)}$ applying the EFT+FBA+SPS, EFT+FBA+SPS, and M-EFT+FBA+SPS methods.

In Figure 7 we show simulation results for the proposed Mode 1 HOSVD SECSI with left-hand matrix slices applying the MuDe method with $K = 30$. Note, that the ideal case with known **A** and Γ is a reference to the smallest error in noisy scenarios. However, in practice, **A** and Γ must be estimated. Observe that, by inspecting the ideal cases with and without MuDe, if the tensor had higher dimensions, then the gain of denoising would be even higher. We can observe a performance gain when applying MuDe to the sub-tensors, since the MOS methods EFT+FBA+SPS, M-EFT+FBA+SPS, and MDL+FBA+SPS curves show a lower error when combined with MuDe. Besides, since the sub-tensor approach attempts to generate pseudo-static scenarios from dynamic ones, the proposed Mode 1 HOSVD SECSI with the left-hand matrix method achieves an accurate matrix separation, thus achieving improved estimates of the factor matrices.

VI. CONCLUSION

State-of-the-art tensor-based TDE methods are not suitable for scenarios with a time-varying number of multipath components. To overcome this limitation, we proposed a tensor-based framework capable of performing model order estimation and factor decomposition for time-delay estimation in dynamic multipath scenarios. The proposed approach is applicable in time-varying multipath environments and selects the most suitable MOS scheme. To perform high accuracy factor decomposition, we exploit the model order estimates for each slice to group the slices into sub-tensors.

Since, by creating sub-tensors, we achieve pseudo-static sub-scenarios, we obtain a model order larger than the

number of epochs. Therefore, the previous state-of-the-art CPD-GEVD and HOSVD SECSI are no longer suitable for dynamic multipath scenarios. We have shown that the proposed Mode 1 HOSVD SECSI provides reliable and accurate estimates when combined with the created sub-tensors. Furthermore, due to the low power of the NLOS components, the NLOS components may be identified as noise when performing MOS. Consequently, the PoD is smaller in case the signals are strongly correlated. Therefore, we have shown that by combining accurate and robust MOS methods with tensor factorization techniques, we obtain more accurate TDE of the LOS signal.

Combining the proposed Mode 1 HOSVD SECSI with MuDe, an additional performance gain can be achieved due to the successful denoising of the generated sub-tensors. Finally, if we increased the number of dimensions and the size of those dimensions, we would obtain an even higher performance gain.

REFERENCES

[1] M. S. Braasch and A. J. van Dierendonck, "GPS receiver architectures and measurements," *Proc. IEEE*, vol. 87, no. 1, pp. 48–64, Jan. 1999.

[2] R. D. J. Van Nee, "Spread-spectrum code and carrier synchronization errors caused by multipath and interference," *IEEE Trans. Aerosp. Electron. Syst.*, vol. 29, no. 4, pp. 1359–1365, Oct. 1993.

[3] J. J. Spilker, P. Axelrad, B. W. Parkinson, and P. Enge, *Global Positioning System: Theory Applicarion*, vol. 1. Reston, VA, USA: American Institute of Aeronautics and Astronautics, 1996.

[4] M. Sgammini, F. Antreich, L. Kurz, M. Meurer, and T. Noll, "Blind adaptive beamformer based on orthogonal projections for GNSS," in *Proc. GNSS*, Nashville, TN, USA, Sep. 2012, pp. 1–4.

[5] F. Fohlmeister, A. Iliopoulos, M. Sgammini, F. Antreich, and J. A. Nossek, "Dual polarization beamforming algorithm for multipath mitigation in GNSS," *Signal Process.*, vol. 138, pp. 86–97, Sep. 2017.

[6] F. Antreich, J. A. Nossek, G. Seco-Granados, and A. L. Swindlehurst, "The extended invariance principle for signal parameter estimation in an unknown spatial field," *IEEE Trans. Signal Process.*, vol. 59, no. 7, pp. 3213–3225, Jul. 2011.

[7] F. Antreich, J. A. Nossek, and W. Utschick, "Maximum likelihood delay estimation in a navigation receiver for aeronautical applications," *Aerosp. Sci. Technol.*, vol. 12, no. 3, pp. 256–267, Apr. 2008.

[8] H. Qin, X. Xue, and Q. Yang, "GNSS multipath estimation and mitigation based on particle filter," *IET Radar, Sonar Navigat.*, vol. 13, no. 9, pp. 1588–1596, Sep. 2019.

[9] N. Chang, X. Hong, W. Wang, and Z. Wang, "Joint delay and angle estimation for GNSS multipath signals based on spatial and frequential smoothing," in *Proc. 14th IEEE Int. Conf. Signal Process. (ICSP)*, Aug. 2018, pp. 203–207.

[10] B. Hammoud, F. Antreich, J. A. Nossek, J. Costa, and A. Almeida, "Tensor-based approach for time-delay estimation," in *Proc. 20th Int. ITG Workshop Smart Antennas*, Mar. 2016, pp. 1–7.

[11] M. Haardt, F. Roemer, and G. Del Galdo, "Higher-order SVD-based subspace estimation to improve the parameter estimation accuracy in multidimensional harmonic retrieval problems," *IEEE Trans. Signal Process.*, vol. 56, no. 7, pp. 3198–3213, Jul. 2008.

[12] T.-J. Shan, M. Wax, and T. Kailath, "On spatial smoothing for direction-of-arrival estimation of coherent signals," *IEEE Trans. Acoust., Speech, Signal Process.*, vol. 33, no. 4, pp. 806–811, Aug. 1985.

[13] P. R. B. Gomes, A. L. F. de Almeida, J. P. C. L. da Costa, J. C. M. Mota, D. V. de Lima, and G. Del Galdo, "Tensor-based methods for blind spatial signature estimation in multidimensional sensor arrays," *Int. J. Antennas Propag.*, vol. 2017, pp. 1–11, Oct. 2017.

[14] D. V. de Lima, J. P. C. L. da Costa, J. P. A. Maranhao, and R. T. de Sousa, "High resolution time-delay estimation via direction of arrival estimation and Khatri-Rao factorization for multipath mitigation," in *Proc. 11th Int. Conf. Signal Process. Commun. Syst. (ICSPCS)*, Berlin, Germany, Dec. 2017, pp. 1–7.

[15] D. V. de Lima, J. P. C. L. da Costa, F. Antreich, R. K. Miranda, and G. Del Galdo, "Time-delay estimation via CPD-GEVD applied to tensor-based GNSS arrays with errors," in *Proc. IEEE 7th Int. Workshop Comput. Adv. Multi-Sensor Adapt. Process. (CAMSAP)*, Dec. 2017, pp. 1–5.

[16] M. da Rosa Zanatta, R. K. Miranda, J. P. C. L. da Costa, F. Antreich, and D. V. Lima, "Antenna array based receivers for third generation global positioning system," in *Proc. Workshop Commun. Netw. Power Syst. (WCNPS)*, Nov. 2017, pp. 1–4.

[17] (2013). *Interface specification IS-GPS-800D*. [Online]. Available: http://www.gps.gov/technical/icwg/IS-GPS-800D.pdf

[18] F. D. Cote, I. N. Psaromiligkos, and W. J. Gross, "GNSS modulation: A unified statistical description," *IEEE Trans. Aerosp. Electron. Syst.*, vol. 47, no. 3, pp. 1814–1836, Jul. 2011.

[19] F. Macchi, "Development and testing of an L1 combined GPS-Galileo software receiver," Ph.D. dissertation, Dept. Geomatics Eng., Univ. Calgary, Calgary, AB, Canada, 2010. [Online]. Available: http://www.geomatics.ucalgary.ca/graduatetheses

[20] M. da Rosa Zanatta, F. L. Lópes de Mendonça, F. Antreich, D. V. de Lima, R. Kehrle Miranda, G. Del Galdo, and J. P. C. L. da Costa, "Tensor-based time-delay estimation for second and third generation global positioning system," *Digit. Signal Process.*, vol. 92, pp. 1–19, Sep. 2019.

[21] F. Roemer and M. Haardt, "A semi-algebraic framework for approximate CP decompositions via simultaneous matrix diagonalizations (SECSI)," *Signal Process.*, vol. 93, no. 9, pp. 2722–2738, Sep. 2013.

[22] D. V. de Lima, M. D. R. Zanatta, J. P. C. L. da Costa, R. T. de Sousa Jr., and M. Haardt, "Robust tensor-based techniques for antenna array-based GNSS receivers in scenarios with highly correlated multipath components," *Digit. Signal Process.*, vol. 101, Jun. 2020, Art. no. 102715.

[23] C. C. R. Garcez, D. V. de Lima, R. K. Miranda, F. Mendonça, J. P. C. L. da Costa, A. L. F. de Almeida, and R. T. de Sousa, "Tensor-based subspace tracking for time-delay estimation in GNSS multi-antenna receivers," *Sensors*, vol. 19, no. 23, p. 5076, Nov. 2019.

[24] J. P. C. L. da Costa, M. Haardt, F. Romer, and G. Del Galdo, "Enhanced model order estimation using higher-order arrays," in *Proc. Conf. Rec. Forty-First Asilomar Conf. Signals, Syst. Comput.*, Nov. 2007, pp. 412–416.

[25] J. Grouffaud, P. Larzabal, and H. Clergeot, "Some properties of ordered eigenvalues of a Wishart matrix: Application in detection test and model order selection," in *1996 IEEE Int. Conf. Acoust., Speech, Signal Process. Conf. Proc.*, vol. 5, May 1996, pp. 2463–2466.

[26] E. Radoi and A. Quinquis, "A new method for estimating the number of harmonic components in noise with application in high resolution radar," *EURASIP J. Appl. Signal Process.*, vol. 2004, pp. 1177–1188, Jan. 2004.

[27] R. Badeau, B. David, and G. Richard, "Selecting the modeling order for the ESPRIT high resolution method: An alternative approach," in *Proc. IEEE Int. Conf. Acoust., Speech, Signal Process.*, May 2004, pp. 1–4.

[28] J. Costa, *Parameter Estimation Techniques for Multi-Dimensional Array Signal Processing*. Herzogenrath, Germany: Shaker Verlag, 2010.

[29] P. Closas and C. Fernandez-Prades, "A statistical multipath detector for antenna array based GNSS receivers," *IEEE Trans. Wireless Commun.*, vol. 10, no. 3, pp. 916–929, Mar. 2011.

[30] M. T. Brenneman, Y. T. Morton, and Q. Zhou, "GPS multipath detection with ANOVA for adaptive arrays," *IEEE Trans. Aerosp. Electron. Syst.*, vol. 46, no. 3, pp. 1171–1184, Jul. 2010.

[31] P. R. B. Gomes, J. P. C. L. da Costa, A. L. F. de Almeida, and R. T. de Sousa, "Tensor-based multiple denoising via successive spatial smoothing, low-rank approximation and reconstruction for R-D sensor array processing," *Digit. Signal Process.*, vol. 89, pp. 1–7, Jun. 2019.

[32] L. N. Trefethen and D. B. III, *Numerical Linear Algebra*. Philadelphia, PA, USA: SIAM, 1997.

[33] J. Selva Vera, "Efficient multipath mitigation in navigation systems," Ph.D. dissertation, Dept. Signal Theory Commun., Univ. Politecnica de Catalunya, Barcelona, Spain, 2003.

[34] A. Quinlan, J.-P. Barbot, P. Larzabal, and M. Haardt, "Model order selection for short data: An exponential fitting test (EFT)," *EURASIP J. Adv. Signal Process.*, vol. 2007, no. 1, p. 201, Dec. 2006.

[35] T. Fu and X. Gao, "Simultaneous diagonalization with similarity transformation for non-defective matrices," in *Proc. IEEE Int. Conf. Acoust. Speed Signal Process. Proc.*, May 2006, p. 4.

[36] J.-F. Cardoso and A. Souloumiac, "Jacobi angles for simultaneous diagonalization," *SIAM J. Matrix Anal. Appl.*, vol. 17, no. 1, pp. 161–164, Jan. 1996.

[37] J. P. C. L. da Costa, D. Schulz, F. Roemer, M. Haardt, and J. A. Apolinaario, "Robust R-D parameter estimation via closed-form PARAFAC in kronecker colored environments," in *Proc. 7th Int. Symp. Wireless Commun. Syst.*, Sep. 2010, pp. 115–119.

[38] D. V. de Lima, J. P. C. L. da Costa, J. P. A. Maranhao, and R. T. de Sousa, "Time-delay estimation via procrustes estimation and Khatri-Rao factorization for GNSS multipath mitigation," in *Proc. 11th Int. Conf. Signal Process. Commun. Syst. (ICSPCS)*, Dec. 2017, pp. 1–7.

[39] M. Zanatta, D. Lima, J. Costa, R. Miranda, F. Antreich, and R. Junior, "Técnica tensorial de Estimaço de atraso para GPS de segunda e terceira Geraço," in *Proc. Simpósio Brasileiro de Telecomunicaçes e Processamento de Sinais*, 2018, pp. 1–4.

MATEUS DA ROSA ZANATTA (Graduate Student Member, IEEE) received the Diploma degree in information systems from the Federal University of Santa Maria (UFSM), Brazil, in 2015, and the M.Sc. degree in mechatronic systems from the University of Brasília (UnB), Brazil, in 2018, where he is currently pursuing the Ph.D. degree, researching on multilinear algebra techniques applied to array-based GNSS receivers. In 2016, he was a Visitor Student with the Ilmenau University of Technology (TU Ilmenau), Germany.

JOÃO PAULO CARVALHO LUSTOSA DA COSTA (Senior Member, IEEE) received the Diploma degree in electronic engineering from the Military Institute of Engineering (IME), Rio de Janeiro, Brazil, in 2003, the M.Sc. degree in telecommunications from the University of Brasília (UnB), Brazil, in 2006, and the Ph.D. degree in electrical and information engineering from the Ilmenau University of Technology (TU Ilmenau), Germany, in 2010. From 2010 to 2019, he coordinated the Laboratory of Array Signal Processing (LASP) and several research projects. For instance, from 2014 to 2019, he coordinated the main project related to distance learning courses at the National School of Public Administration and a Special Visiting Researcher (PVE) project related to satellite communication and navigation with the German Aerospace Center (DLR) supported by the Brazilian Government. Since March 2019, he has been a Senior Development Engineer at the EFS in the area of autonomous driving. Moreover, since October 2019, he has been a Lecturer at the Ingolstadt University of Applied Sciences in the area of autonomous vehicles. He has published more than 170 scientific publications and patents. He has obtained six best paper awards in international conferences. His research interests include autonomous vehicles, beyond 5G, GNSS, and adaptive and array signal processing.

FELIX ANTREICH (Senior Member, IEEE) received the Diploma degree in electrical engineering and the Doktor-Ingenieur (Ph.D.) degree from the Technical University of Munich (TUM), Munich, Germany, in 2003 and 2011, respectively. From 2003 to 2016, he was an Associate Researcher with the Department of Navigation, Institute of Communications and Navigation of the German Aerospace Center (DLR), Wessling, Germany. From 2016 to 2018, he was a Visiting Professor with the Department of Teleinformatics Engineering (DETI), Federal University of Ceará (UFC), Fortaleza, Brazil. Since July 2018, he has been a Professor with the Department of Telecommunications, Division of Electronics Engineering, Aeronautics Institute of Technology (ITA), São José dos Campos, Brazil. His research interests include sensor array signal processing for global navigation satellite systems (GNSS) and wireless communications, estimation theory, wireless sensor networks, positioning, localization, and signal design for synchronization.

MARTIN HAARDT (Fellow, IEEE) received the Diplom-Ingenieur (M.S.) degree from the Ruhr-University Bochum, Germany, in 1991, and the Doktor-Ingenieur (Ph.D.) degree from the Munich University of Technology, in 1996, after studying electrical engineering at the Ruhr-University Bochum and Purdue University, West Lafayette, IN, USA. He has been a Full Professor with the Department of Electrical Engineering and Information Technology and the Head of the Communications Research Laboratory, Ilmenau University of Technology, Germany, since 2001. In 1997, he joined Siemens Mobile Networks, Munich, Germany, where he was responsible for strategic research on third-generation mobile radio systems. From 1998 to 2001, he was the Director for International Projects and University Cooperations in the mobile infrastructure business of Siemens, Munich, where his work focused on mobile communications beyond the third generation. During his time at Siemens, he also taught in the International Master of Science in Communications Engineering Program at the Munich University of Technology. In the Fall of 2006 and the Fall of 2007, he was a Visiting Professor with the University of Nice, Sophia-Antipolis, France, and the University of York, U.K., respectively. From 2012 to 2017, he also served as an Honorary Visiting Professor with the Department of Electronics, University of York, U.K., in 2019, as an Invited Professor at the Université de Lorraine, Nancy, France. His research interests include wireless communications, array signal processing, high-resolution parameter estimation, as well as numerical linear and multilinear algebra. In 2018, he was named an IEEE Fellow "for contributions to multi-user MIMO communications and tensor-based signal processing." He has received the 2009 Best Paper Award from the IEEE Signal Processing Society, the Vodafone (formerly Mannesmann Mobilfunk) Innovations-Award for outstanding research in mobile communications, the ITG Best Paper Award from the Association of Electrical Engineering, Electronics, and Information Technology (VDE), and the Rohde & Schwarz Outstanding Dissertation Award. From 2011 to 2019, he was an elected member of the Sensor Array and Multichannel (SAM) Technical Committee of the IEEE Signal Processing Society, where he served as the Vice Chair, from 2015 to 2016; Chair, from 2017 to 2018; and Past Chair in 2019. Since 2020, he has been an elected member of the Signal Processing Theory and Methods (SPTM) Technical Committee of the IEEE Signal Processing Society. Moreover, he has served as the Technical Co-Chair for PIMRC 2005, Berlin, Germany; ISWCS 2010 in York, U.K.; the European Wireless 2014, Barcelona, Spain; as well as the Asilomar Conference on Signals, Systems, and Computers 2018, USA. He has also served as the General Co-Chair for WSA 2013, Stuttgart, Germany; ISWCS 2013, Ilmenau, Germany; CAMSAP 2013, Saint Martin, French Antilles; WSA 2015, Ilmenau; SAM 2016, Rio de Janeiro, Brazil; CAMSAP 2017, Curacao, Dutch Antilles; SAM 2020, Hangzhou, China; as well as the Asilomar Conference on Signals, Systems, and Computers 2021, USA. He has served as an Associate Editor for the IEEE Transactions on Signal Processing from 2002 to 2006 and from 2011 to 2015, the IEEE Signal Processing Letters from 2006 to 2010, the *Research Letters in Signal Processing* from 2007 to 2009, the *Hindawi Journal of Electrical and Computer Engineering* since 2009, and the *EURASIP Signal Processing Journal* from 2011 to 2014. He has been serving as a Senior Editor for the IEEE Journal of Selected Topics in Signal Processing (JSTSP) since 2019 and as a Guest Editor for the *EURASIP Journal on Wireless Communications and Networking* as well as the IEEE JSTSP.

GORDON ELGER received the Ph.D. degree in physics from the Free University of Berlin, Berlin, Germany, in 1998. Since 2013, he has been a Professor with the University of Applied Science in Ingolstadt (THI) for electronic manufacturing technologies. In 2016, he became a Research Professor and has been working part-time with the Fraunhofer Institute for Mobility and Infrastructure (Fraunhofer-IVI), since 2018, to establish the Research Application Center in Ingolstadt as a department from Fraunhofer-IVI. After his Ph.D. degree, he worked as a Scientific Coworker with the Fraunhofer Institute for Reliability and Microintegration (Fraunhofer-IZM Berlin) in the field of optoelectronic, high frequency, and sensor packaging. He joined the Hymite GmbH, Berlin, where he became the Team Leader of the backend team developing hermetic packaging technologies for optoelectronic and MEMS. In 2005, he joined the Central RD Department, Electrolux, Italy, as the Manager of the team for heat and mass transfer, applying computational fluid dynamic and finite element simulations. He returned to Germany and worked with Philips in the Automotive Center, Aachen, focusing on LED packaging and thermal analysis of LED modules. His research at THI was focused on optoelectronic- and sensor packaging for automotive applications and reliability and lifetime assessment using physical and data-driven modeling. His secondary focus was on sensor signal processing and data fusion for automotive applications, i.e., autonomous driving.

FÁBIO LÚCIO LOPES DE MENDONÇA received the Diploma degree in data processing from the Catholic University of Brasília (UCB), in 2004, and the M.Sc. and Ph.D. degrees in electrical engineering from the University of Brasília (UnB), in 2008 and 2019, respectively. He was a Consultant in the computer network, software engineering, and project management, and also the Project Manager with the Decision-Making Technology Laboratory (LATITUDE), UnB, where he is currently an Assistant Professor with the Network Engineering Course and an Assistant Professor with the Projeção College (UniProjeção).

RAFAEL TIMÓTEO DE SOUSA, JR. (Senior Member, IEEE) received the bachelor's degree in electrical engineering from the Federal University of Paraíba—UFPB, Campina Grande, Brazil, in 1984, the master's degree in computing and information systems from the Ecole Supérieure d'Electricité–Supélec, Rennes, France, from 1984 to 1985, and the Ph.D. degree in telecommunications and signal processing from the University of Rennes 1, Rennes, in 1988. He was a Visiting Researcher with the Group for Security of Information Systems and Networks (SSIR), Ecole Supérieure d'Electricité–Supélec, from 2006 to 2007. He worked in the private sector from 1988 to 1996. Since 1996, he has been a Network Engineering Associate Professor with the Electrical Engineering Department, University of Brasília, Brazil, where he is the Coordinator of the Professional Post-Graduate Program on Electrical Engineering (PPEE) and supervises the Decision Technologies Laboratory (LATITUDE). He is the Chair of the IEEE VTS Centro-Norte Brasil Chapter (IEEE VTS Chapter of the Year 2019) and the IEEE Centro-Norte Brasil Blockchain Group. His professional experience includes research projects with Dell Computers, HP, IBM, Cisco, and Siemens. He has coordinated research, development, and technology transfer projects with the Brazilian Ministries of Planning, Economy, and Justice, as well as with the Institutional Security Office of the Presidency of Brazil, the Administrative Council for Economic Defense, the General Attorney of the Union, and the Brazilian Union Public Defender. He has received research grants from the Brazilian research and innovation agencies CNPq, CAPES, FINEP, RNP, and FAPDF. He has developed research in cyber, information and network security, distributed data services and machine learning for intrusion and fraud detection, as well as signal processing, energy harvesting, and security at the physical layer.

• • •